

## Device Optimization of a High-Efficiency Lead-Free Perovskite-Perovskite Tandem Solar Cell

Mohammad Aminul Islam<sup>1\*</sup>, Md Jakir Hossen<sup>1</sup>, Hairul Mardiah Hamzah<sup>1</sup>, Sharifah Fatmadiana Wan Muhammad Hatta<sup>1</sup>, Norhayati Binti Soin<sup>1</sup> and Md. Bulu Rahman<sup>2</sup>

<sup>1</sup>Department of Electrical Engineering, Faculty of Engineering, Universiti Malaya, Jalan Universiti, Kuala Lumpur, Malaysia

<sup>2</sup>Bangabandhu Sheikh Mujibur Rahman Science and Technology University, Gopalganj, 8100, Bangladesh

\*Corresponding Author: Mohammad Aminul Islam, Department of Electrical Engineering, Faculty of Engineering, Universiti Malaya, Jalan Universiti, Kuala Lumpur, Malaysia.

Received: January 20, 2023

Published: February 16, 2023

© All rights are reserved by **Mohammad Aminul Islam, et al.**

### Abstract

Perovskite based tandem solar cell topologies have garnered a lot of interest in the field of photovoltaic for surpassing the single-cell efficiency limit and achieving the power conversion efficiency (PCE) beyond 30%. However, the PCE as well as stability of tandem solar cells may severely affected by the optical and electrical mismatching and choosing the wrong carrier transport materials, thus it is important to be optimized the active layers' parameters for achieving optimum performance. In this study, the SCAPS 1D device simulation tool was utilized to optimize a highly efficient lead-free perovskite-perovskite tandem solar cell (PPTSC). The absorber material in the tandem structure was Cs<sub>2</sub>AgBi<sub>0.75</sub>Sb<sub>0.25</sub>Br<sub>6</sub> (E<sub>g</sub> = 1.80 eV) in the top cell and FAMASnGeI<sub>3</sub> (E<sub>g</sub> = 1.40 eV) in the bottom cell. The optimized device shows a promising PCE of 28.87% with high Voc of 2.08 V. The significant impact of device temperature has also been investigated and the temperature gradient found to be -0.098%/oC. We believe that the proposed device has enormous potential for the fabrication of a highly efficient PPTSC, and achieving successful commercialization.

**Keywords:** Perovskite-perovskite Tandem Solar Cell; Lead-free; SCAPS 1D; High Efficiency; Absorber Layer; Temperature Gradient

### Introduction

Solar PV technology has advanced rapidly over the last few decades as a result of technological advancements and an increase in commercial manufacturing [1]. Additionally, global energy demand is rising at the same time. To reduce energy demand and reliance on fossil fuels, the efficiency of the PV solar cell should be greater than 30%. The Shockley-Queisser (SQ) limit confirmed that it is not possible to obtain using single junction solar cells [2]. The performance is primarily limited by two factors: first, optical loss, which occurs when photon energies less than the bandgap cannot be absorbed, and second, thermalization loss. When photon energy exceeds the energy required to form free electron-hole pairs, carriers thermalize instead of contributing to the device's usable output. These losses can be reduced by stacking different

solar cells with different semiconducting materials of the appropriate bandgap so that the incident spectrum is absorbed separately by the stacks. Wide/narrow bandgap materials are used for the top/bottom subcell in this approach to effectively use lower wavelength photons alongside higher wavelength photons. Jacksoin proposed the concept for the first time in 1955 [3]. Following that, several researchers then conducted theoretical and experimental studies on multijunction concentrator cells, also known as cascade or tandem cells [4,5]. Consequently, all-perovskite tandem solar cells have recently received a lot of attention as a way to improve device performance [6].

The simulation of a novel structure lead-free all-perovskite tandem solar cell based on double perovskite Cs<sub>2</sub>AgBi<sub>0.75</sub>Sb<sub>0.25</sub>Br<sub>6</sub>

( $E_g = 1.80$  eV) and FAMASnGeI<sub>3</sub> ( $E_g = 1.40$  eV) is included in this study. The Cs<sub>2</sub>AgBi<sub>0.75</sub>Sb<sub>0.25</sub>Br<sub>6</sub> double halide perovskites have demonstrated some desirable properties, including excellent stability in the open air and appropriate bandgaps [7]. The impact of both absorber layer thicknesses on the performance of a stand-alone solar cell has been studied. A novel all-perovskite tandem solar cell structure with inorganic ETL and HTL, such as SnO<sub>2</sub> and Cu<sub>x</sub>O, is proposed in this study. It should be noted that the suitable ETL and HTL layer is essential for proper charge facilitation from the perovskite layer to the electrodes. The device was simulated and investigated using the one-dimensional SCAPS (Solar Cell Capacitance Simulator version 3.3.07) tool. SCAPS is widely used for perovskite solar cell simulation due to its inherent ability to simulate defect configurations (bulk and interface) and energy distributions (single, uniform, Gaussian). Furthermore, it has enabled the changing of the work function of the contact materials as well as the use of optical filters for reflection and transmission functions. Several publications also show a successful application of the perovskite solar cell with outstanding photovoltaic performance using SCAPS 1D [8-10]. As a result, numerical modeling of a perovskite solar cell with SCAPS-1D is an appropriate technique for advancing the development of perovskites in photovoltaics. It should be noted that the perovskite-perovskite tandem solar cell (PPTSC) is still in its early stages of development. We believe that the detailed simulation of a Pb-free PPTSC described in this paper

will pave the way for the future development of non-toxic solar cells with high efficiency.

### Device structure and parameters

To understand the photovoltaic performance of the lead-free all-perovskite tandem solar cell, initially, the device performance of single layer perovskite solar cell based on Cs<sub>2</sub>AgBi<sub>0.75</sub>Sb<sub>0.25</sub>Br<sub>6</sub> and FAMASnGeI<sub>3</sub> layers has been investigated. The device structures for standalone perovskite and tandem perovskite solar cell has been shown in figure 1(a), (b) and (c).

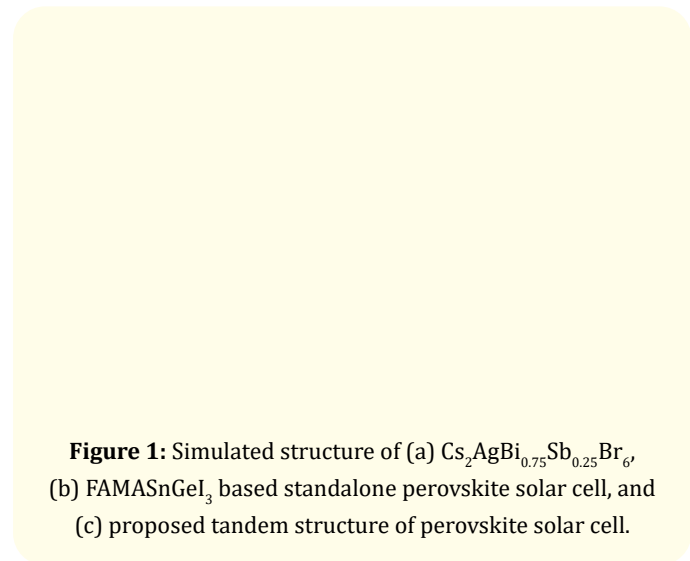


**Figure 1:** Simulated structure of (a) Cs<sub>2</sub>AgBi<sub>0.75</sub>Sb<sub>0.25</sub>Br<sub>6</sub>, (b) FAMASnGeI<sub>3</sub> based standalone perovskite solar cell, and (c) proposed tandem structure of perovskite solar cell.

Parameter	Cu <sub>x</sub> O	FAMASnGeI <sub>3</sub>	Cs <sub>2</sub> AgBi <sub>0.75</sub> Sb <sub>0.25</sub> Br <sub>6</sub>	SnO <sub>2</sub>	FTO
Band Gap, E <sub>g</sub> (eV)	2.1	1.40	1.80	3.6	3.50
Electron affinity, X <sub>e</sub> (eV)	3.4	3.67	3.98	4.5	4.00
Thickness, w (nm)	300	400	400	70	200
Electron mobility, μ <sub>n</sub> (cm <sup>2</sup> /Vs)	30	2.0	1.62 × 10 <sup>5</sup>	100	20
Hole mobility, μ <sub>p</sub> (cm <sup>2</sup> /Vs)	30	2.0	1.010 × 10 <sup>5</sup>	25	10
Permittivity, ε <sub>r</sub>	7.5	8.2	10.0	9.0	9.0
Effective density of states (Conduction Band), N <sub>c</sub> (cm <sup>-3</sup> )	2.5 × 10 <sup>19</sup>	2.2 × 10 <sup>18</sup>	1 × 10 <sup>16</sup>	2.2 × 10 <sup>18</sup>	2.2 × 10 <sup>18</sup>
Effective density of states (Valence band), N <sub>v</sub> (cm <sup>-3</sup> )	2.5 × 10 <sup>19</sup>	1.8 × 10 <sup>19</sup>	1 × 10 <sup>16</sup>	1.8 × 10 <sup>19</sup>	1.8 × 10 <sup>19</sup>
Electrothermalvelocity (cm/s)	1 × 10 <sup>7</sup>				
Hole thermalvelocity (cm/s)	1 × 10 <sup>7</sup>				
Carrier density of the acceptor, N <sub>a</sub> (cm <sup>-3</sup> )	3 × 10 <sup>16</sup>	0	1 × 10 <sup>9</sup>	0	0
Carrier density of the Donor, N <sub>d</sub> (cm <sup>-3</sup> )	3 × 10 <sup>14</sup>	1 × 10 <sup>13</sup>	1 × 10 <sup>9</sup>	1 × 10 <sup>20</sup>	1 × 10 <sup>18</sup>

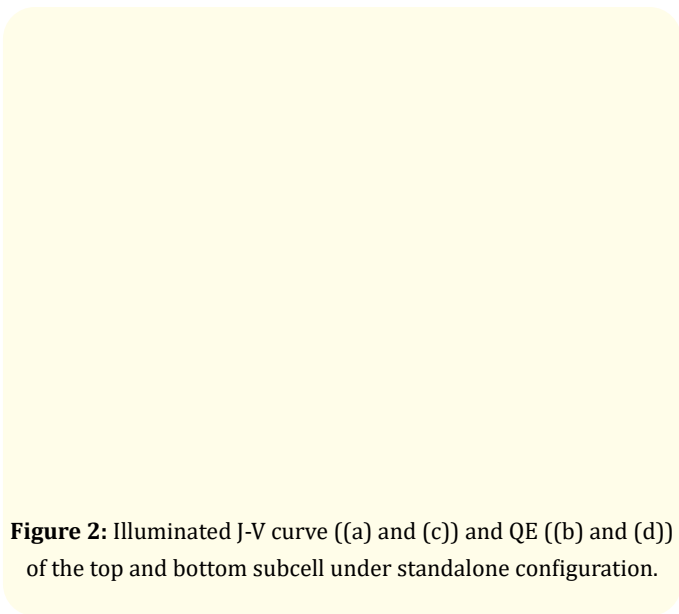
**Table 1:** The initial layer parameters adopted for this study (symbols have their usual meanings).

Table 2 shows the initial device parameters which we have taken for the simulation of single-layer perovskite solar cells and tandem solar cells. The parameters of the different layers have been adopted from the different published works [11-16].

## Results and Discussion

### Calibration of top cell and bottom cell

At first, individual solar cells with single perovskite layers with wide band gaps ( $\text{Cs}_2\text{AgBi}_{0.75}\text{Sb}_{0.25}\text{Br}_6$ ) and low band gaps ( $\text{FAMASnGeI}_3$ ) perovskite were simulated. The current density-voltage (J-V) curve and external quantum efficiency (EQE) of the standalone top and bottom cells are obtained and shown in figure 2(a), 2(b), 2(c), and 2(d). Furthermore, the insets of figures 2(a) and (c) provide an overview of the PV parameters of the simulated devices, such as  $J_{sc}$ , VOC, FF, and power conversion efficiency (PCE). Furthermore, both cells had more than 80% QE at 400 nm, whereas the top cell's QE drops below 60% at wavelengths greater than 650 nm. This is due to the perovskite top cell solar cell's large bandgap (1.8 eV). The QE of the simulated QE for 1.8 eV top-cell is quite close to the experimental device reported elsewhere [17]. As illustrated in Figure 2(c) and 2(d), the cut-off wavelength for QE is nearly 50% higher in the bottom subcell along with larger spectrum width, resulting in better spectrum utilization and therefore higher  $J_{sc}$  is observed for the bottom cell as shown in figure 2(b).



**Figure 2:** Illuminated J-V curve ((a) and (c)) and QE ((b) and (d)) of the top and bottom subcell under standalone configuration.

### Absorber layer optimization

Before investigating the performance of the perovskite-perovskite tandem structure, the top and bottom cells were evaluated separately via altering the absorber layers' thickness. Figures 3(a) and (b) show the efficiency at various absorber layer thicknesses of individual (top and bottom) solar cells, and it can be seen a significant impact of active layer thickness on cell efficiency. Figure 3(a) shows that the device performance is increased until the thickness of the top cell's absorber layer is 400 nm, with a quantitative increase of 12.85%. The improvement is attributed to improved optical absorption in the device's active region, which promotes the electron-hole pairs generation and the subsequent separation. For the bottom cell, device performance is also increased until 200 nm of the  $\text{FAMASnGeI}_3$  absorber layer and the average increase of efficiency is 12.85%. Both cells are showing decreasing trends of the performance parameters after the increase of the active layer's thickness. The decline in performance could be attributed to an increase in resistance as absorber thickness increases [18]. It should be noted that as the active layer thickness increases, so does the device's overall series resistance. Furthermore, the possibility of recombination increases because charges must travel a greater distance for diffusion in a thicker absorber layer. As a result, after a certain thickness value, efficiency decreases. This finding agrees with the experimental findings of Correa-Baena., *et al.* [19]. As a result, the ideal thicknesses for the  $\text{Cs}_2\text{AgBi}_{0.75}\text{Sb}_{0.25}\text{Br}_6$  and  $\text{FAMASnGeI}_3$ -based perovskite layers are 400 nm and 200 nm, respectively. Similar results have been reported elsewhere [11] for different structures of  $\text{FAMASnGeI}_3$ -based solar cells.

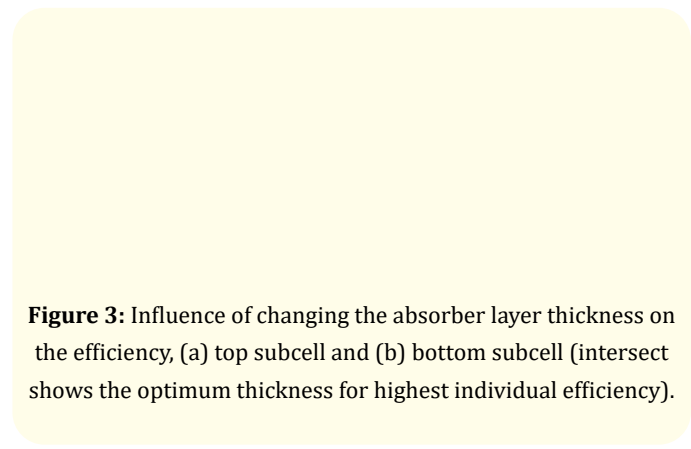


**Figure 3:** Influence of changing the absorber layer thickness on the efficiency, (a) top subcell and (b) bottom subcell (intersect shows the optimum thickness for highest individual efficiency).

After the individual solar cells have been optimized, they are connected in series for tandem application, as shown in Figure 1(c). Figure 4 depicts the I-V curve discovered through simulation. Figure 4 shows that the tandem solar cell's current density is nearly equal to the current density of the top cell, while open circuit voltage is the sum of the two sub-cells. Two-terminal tandem solar cells behave electrically like two diodes connected in series, so an equal amount of current must always flow through each cell. As a result, the cell with the lowest  $J_{sc}$  values (here, the top cell) serves as a limiting cell for the overall  $J_{sc}$  of the tandem device. Furthermore, the total voltage drop across the tandem device is equal to the sum of the individual voltage drops of each cell [20]. Consequently, the thickness of the active layer in the top and bottom cells greatly influences tandem device performance, and top and bottom cell mismatches result in subpar tandem device performance. To get the best performance from the tandem device, the thickness of the top and bottom cells must be tuned to have the same  $J_{sc}$  value and to enable the same tunnel recombination junctions [21-24]. Furthermore, increasing the top cell's thickness above the optimal level results in increased parasitic absorption in the top cell and decreased optical coupling in the bottom cell, lowering the tandem device's total  $J_{sc}$  value. Furthermore, decreasing the thickness of the top cell below the optimal value reduces absorption in the top, which has the same effect as decreasing  $J_{sc}$ . Current matching conditions are obtained to produce the identical  $J_{sc}$  value in the top and bottom cells using optical coupling.

The estimated filtered spectra were used to investigate photon optical coupling in the two sub-cells. When the thickness of the top subcell's perovskite layer is less, the bottom cell receives more photocurrent. In this case, the top cell is illuminated with the AM1.5 spectrum, and the transmitted spectrum,  $S(\lambda)$  by the top cell is calculated using the absorption coefficient and thickness of all layers using the following equation.

$$S(\lambda) = S_0(\lambda) \cdot \exp[-\alpha(\lambda) \cdot d] \quad (1)$$

Here,  $S_0(\lambda)$  represents the incident AM1.5 spectrum,  $\alpha$  is the absorption coefficient, and  $d$  represents the thickness of the top cell's perovskite material. Interfacial reflection losses and absorption by other layers, such as FTO,  $\text{SnO}_2$ , and  $\text{Cu}_x\text{O}$ , have been ignored for simplicity. The estimated filtered transmitted spectrum by top cells with different absorber layer thicknesses is shown in figure 5(a). The power of the filtered transmitted spectrum is reduced when the absorber layer in the top cell is thicker, especially below 700 nm wavelengths. This is due to increased absorption in top cells with thick absorber layers.

**Figure 4:** J-V curve of the standalone top, standalone bottom, and tandem cell.

**Figure 5:** (a) Transmitted spectrum by the top sub-cell for different thicknesses of the absorber of the top sub-cell, (b)  $J_{sc}$  for top and bottom cell at a different thickness of the top and bottom perovskite (100–500 nm) (the optimum pairing is at around 400 nm of top cell perovskite indicated by arrow sign), and (c) J-V curve of the top cell, bottom cell after fed with the filtered spectrum and tandem cell (current matching condition).

It has been found that as the top sub-cell thickness approaches 400 nm, the transmitted photocurrent decreases. As previously stated, if the thickness of the top-subcell falls below a certain threshold, absorption in the top cell and overall  $J_{sc}$  of the tandem cell is reduced. Similarly, if the thickness of the top cell exceeds a certain threshold, absorption in the bottom cell decreases and overall  $J_{sc}$  decreases. Following this fact, we established a current matching condition to obtain the same  $J_{sc}$  value in both sub-cells. We illuminated the bottom cell with the filtered spectra shown in Figure 5(a) to evaluate the PV parameters. The bottom subcell thickness varied from 50 to 500 nm. The  $J_{sc}$  values obtained in this process were used to determine the pairing condition of the tandem device, as shown in Figure 5. (b). The best current matching condition which confirms the higher equal  $J_{sc}$  for both sub-cells is found to be a top-sub-cell thickness of 390 nm and bottom cell thickness of 200 nm, yielding  $J_{sc}$  values equal to 15.49 mA/cm<sup>2</sup> and 15.21 mA/cm<sup>2</sup>. The PV parameters of both Sub-cells under the current matching condition are shown in Table 2. Finally, both sub-cell is connected in series (2T) as shown in Figure 1(c) and the simulated J-V curves for the stand-alone condition and  $J_{sc}$  matched condition are shown in Figure 6(c) and 6(d). From the simulation, the highest efficiency for the tandem has been found to be,  $V_{oc} = 2.08$  V,  $J_{sc} = 15.36$  mA/cm<sup>2</sup>, FF = 81.07%, and efficiency = 28.87%.

PV parameters for the top cell, and bottom cell after fed with the filtered spectrum and tandem cell.

Cell	Jsc (mA/cm <sup>2</sup> )	Voc (V)	FF	PCE (%)
Top cell	15.49	1.19	89.17	17.11
Bottom cell	15.21	0.89	76.99	17.25
Tandem cell	15.36	2.08	81.07	28.87

Table 2

### Effect of temperature

Solar cells are typically employed outdoors where they are exposed to sunlight, which can raise the cell temperature by as much as 60°C. Because of this, numerous investigations have demonstrated that long-term stability is the most challenging task for PSCs. As the temperature impacts are crucial, we simulated the working temperature’s impact on the proposed tandem solar cell. The effect of the working temperature on the efficiency of the tandem solar cell can be seen in figure 6. The rising temperature primarily affects the  $V_{oc}$  and its decay with the increase of temperature leads

to the decrease of efficiency of the solar cell. Particularly, due to its direct relationship with reverse saturation current density ( $J_0$ ), which is also connected to intrinsic carrier concentration ( $n_i$ ),  $V_{oc}$  is decreased. Additionally, a high temperature may generate more excited electrons, which would increase carrier recombination and lower efficiency. The temperature coefficient has also been calculated from Figure 6 and it has been found that the coefficient is -0.098%/°C for the proposed all perovskite Pb-free perovskite solar cells.

Figure 6: Effect of the working temperature on the efficiency of the tandem solar cell.

### Conclusion

In this study, a detail effort was given to optimized perovskite-perovskite Pb-free tandem solar cell through a numerical simulation. At first, to achieve the realistic tandem operation, a current matching condition has been confirmed via alteration of the absorber layers’ thickness in both the top and bottom subcells. Individual cell efficacy has been found to be 17.11% (top) and 17.25% (bottom) under current matching conditions where the optimum thickness for the top and bottom cell absorber layers was found to be 400 nm and 200 nm, respectively. The proposed tandem device has shown an appealing power conversion efficiency of 28.87% with PV parameters  $V_{oc} = 2.08$  V,  $J_{sc} = 15.36$  mA/cm<sup>2</sup>, and FF = 81.07%. The temperature gradient was found to be 0.098%/°C for this device. To further improve conversion efficiency, the influence of tunnel recombination junctions and improvement of the reported device in terms of structural and parametric modification can be done in the future.

## Acknowledgment

The authors would like to acknowledge the Faculty of Engineering, Universiti Malaya for supporting this work through the grant "RMF0423-2021".

## Bibliography

1. Reyes-Belmonte M A. "Quo vadis solar energy research?". *Applied Sciences* 11.7 (2021): 3015.
2. Shockley W and Queisser H J. "Detailed balance limit of efficiency of p-n junction solar cells". *Journal of Applied Physics* 32.3 (1961): 510-519.
3. Wolf M. "Limitations and possibilities for improvement of photovoltaic solar energy converters: Part I: Considerations for earth's surface operation". *Proceedings of the IRE* 48.7 (1961): 1246-1263.
4. Loferski J J. "Theoretical and experimental studies of tandem or cascade solar cells: A review". In Conf. Rec. IEEE Photovoltaic Spec. Conf.; (United States) (No. CONF-820906-). Brown University, Providence, RI (1982).
5. Hutchby JA., et al. "High-efficiency tandem solar cells on single-and poly-crystalline substrates". *Solar Energy Materials and Solar Cells* 35 (1994): 9-24.
6. Jiang F, et al. "A two-terminal perovskite/perovskite tandem solar cell". *Journal of Materials Chemistry A* 4.4 (2016): 1208-1213.
7. Kumar A and Singh S. "Computational simulation of metal doped lead-free double perovskite (Cs<sub>2</sub>AgBi<sub>0.75</sub>Sb<sub>0.25</sub>Br<sub>6</sub>) solar cell using solar cell capacitance simulator". *Materials Today: Proceedings* 44 (2021): 2215-2222.
8. Zhao P, et al. "Device simulation of inverted CH<sub>3</sub>NH<sub>3</sub>PbI<sub>3</sub>-xCl<sub>x</sub> perovskite solar cells based on PCBM electron transport layer and NiO hole transport layer". *Solar Energy* 169 (2018): 11-18.
9. Chakraborty K, et al. "Numerical study of Cs<sub>2</sub>TiX<sub>6</sub> (X= Br<sup>-</sup>, I<sup>-</sup>, F<sup>-</sup> and Cl<sup>-</sup>) based perovskite solar cell using SCAPS-1D device simulation". *Solar Energy* 194 (2019): 886-892.
10. Raoui Y, et al. "Performance analysis of MAPbI<sub>3</sub> based perovskite solar cells employing diverse charge selective contacts: Simulation study". *Solar Energy* 193 (2019): 948-955.
11. Madan J, et al. "Device simulation of 17.3% efficient lead-free all-perovskite tandem solar cell". *Solar Energy* 197 (2020): 212-221.
12. Shamna M S., et al. "Simulation and optimization of CH<sub>3</sub>NH<sub>3</sub>SnI<sub>3</sub> based inverted perovskite solar cell with NiO as Hole transport material". *Materials Today: Proceedings* 33 (2020): 1246-1251.
13. Minemoto T, et al. "Theoretical analysis of band alignment at back junction in Sn-Ge perovskite solar cells with inverted pin structure". *Solar Energy Materials and Solar Cells* 206 (2020): 110268.
14. Jalalian D, et al. "Modeling of a high performance bandgap graded Pb-free HTM-free perovskite solar cell". *The European Physical Journal Applied Physics* 87.1 (2019): 10101.
15. Mandadapu U, et al. "Simulation and analysis of lead based perovskite solar cell using SCAPS-1D". *Indian Journal of Science and Technology* 10.11 (2017): 65-72.
16. Islam M A, et al. "High mobility reactive sputtered CuxO thin film for highly efficient and stable perovskite solar cells". *Crytals* 11.4 (2021): 389.
17. Eperon G E., et al. "Perovskite-perovskite tandem photovoltaics with optimized band gaps". *Science* 354.6314 (2020): 861-865.
18. Singh N, et al. "Numerical simulation of highly efficient lead-free all-perovskite tandem solar cell". *Solar Energy* 208 (2020): 399-410.
19. Correa-Baena J P, et al. "Unbroken perovskite: interplay of morphology, electro-optical properties, and ionic movement". *Advanced Materials* 28.25 (2016): 5031-5037.
20. Burdick J and Glatfelter T. "Spectral response and IV measurements of tandem amorphous-silicon alloy solar cells". *Solar Cells* 18 (1986).
21. Chen B, et al. "Grain engineering for perovskite/silicon monolithic tandem solar cells with efficiency of 25.4%". *Joule* 3.1 (2019): 177-190.



22. Pandey R, *et al.* "Toward the design of monolithic 23.1% efficient hysteresis and moisture free perovskite/c-Si HJ tandem solar cell: a numerical simulation study". *Journal of Micromechanics and Microengineering* 29.6 (2019): 064001.
23. Ramírez Quiroz C O, *et al.* "Interface molecular engineering for laminated monolithic perovskite/silicon tandem solar cells with 80.4% fill factor". *Advanced Functional Materials* 29.40 (2019): 1901476.
24. Sahli F, *et al.* "Fully textured monolithic perovskite/silicon tandem solar cells with 25.2% power conversion efficiency". *Nature Materials* 17.9 (2018): 820-826.
25. Leijtens T, *et al.* "Overcoming ultraviolet light instability of sensitized TiO<sub>2</sub> with meso-super structured organometal tri-halide perovskite solar cells". *Nature Communications* 4.1 (2013): 2885.
26. Han Y, *et al.* "Degradation observations of encapsulated planar CH<sub>3</sub>NH<sub>3</sub>PbI<sub>3</sub> perovskite solar cells at high temperatures and humidity". (2015).
27. Dong L, *et al.* "Elastic properties and thermal expansion of lead-free halide double perovskite Cs<sub>2</sub>AgBiBr<sub>6</sub>". *Computational Materials Science* 141 (2018): 49-58.